INTERNATIONAL JOURNAL OF Telecommunications
AIR DEFENSE COLLEGE

Revolutionizing Stroke Rehabilitation: Dynamic Glove-Based Rehabilitation System Empowered by CNN for Spastic Hands.

Citation: Massoud1 , M.; Mahmoud , G.; Ali, Y.; Abouelwafa ,W.
Inter. Jour. of Telecommunications, ***IJT'2023****, Vol. 04, Issue 01, pp. 01-18, 2024.*
Editor-in-Chief: Youssef Fayed.
Received: 01/03/2024.
Accepted: 08/11/2023.
Published: 04/03/2024.

Mohamed A. Massoud[1,*], Gehan A. Mahmoud[2], Ali W. Y[3], and Wael Abouelwafa Ahmed[1]
*[1]Department of Biomedical Engineering, Faculty of Engineering, Minia University, Minia, 61519, Egypt.
[2]D epartment of Rheumatology and Rehabilitation, Faculty of Medicine, Minia University
3Department of Production Engineering and Mechanical Design, Faculty of Engineering, Minia University, Minia 61111, Egypt.
*Corresponding author(s). E-mail(s): dr.massoud@mu.edu.eg
Contributing authors: wahyos@hotmail.com; gehanabdelwahab@yahoo.com; wael.wafa@minia.edu.eg

Abstract

Hand spasticity poses a significant challenge for stroke survivors, impacting hand functionality and hindering daily activities .

The study introduces a smart rehabilitation system engineered for post-stroke hand spasticity. Comprising four units includes biometric measurement gloves, rehabilitation gloves, a camera, a telecom unit, and a computer unit. Biometric measurement gloves with sensors measure patient features. Data inputs include biometric measurements and camera-captured images. Computer programs consist of a clinical biometric program and a CNN program, specifically ResNet50 architecture. The telecom unit facilitates communication between the computer unit and rehabilittion gloves, doctor section, and patient section. The smart rehabilitation system offers advantages such as user-friendly operation, cost-effectiveness, elimination of physical visits to rehabilitation centers, and exceptional accuracy with a 99% validation accuracy rate and 0.0053 validation loss in the CNN framework. The clinical biometric program is used to analyze programs with high accuracy. This study presents an innovative rehabilitation system. It includes biometric measurement gloves for patient assessment and rehabilitation gloves for hand exercises. Two programs, a clinical biometric program, and an intelligent CNN-based program, diagnose and therapies based on biometric data and image analysis. The mobile application communicates between the system, patients, and healthcare providers.

Keywords: *Spasticity, Dynamic splint, soft gloves, CNN, a smart rehabilitation system.*

1. Introduction

Worldwide, the incidence of stroke has increased resulting in disability and death [1]. Affection of Hand function and activities of daily living (ADL) and independence occurs in many stroke patients [2,3].

Stroke or cerebrovascular disease (CVA) is characterized by interruption of the cerebral circulation at any part by occlusion or rupture of blood vessels [4]. CVA is the main cause of disabilities affecting mid to late adulthood worldwide [4–6]. Post-stroke, the spasticity of upper limbs or lower limbs develops depending on the affected area of cerebral circulation [7, 8]. Spasticity frequently affects the upper limbs as the middle cerebral artery is the most affected artery by stroke [9, 10]. Spasticity resulting from hyperexcitability of the stretch reflex is characterized by

an increase in tonic stretch reflexes and muscle tone with exaggerated tendon jerks [11]. Spasticity of the upper limb in stroke patients poses functional challenges in doing activities of daily living [10].

If spasticity is not treated muscle weakness, muscle atrophy as well as poor hand functional skills occur in the affected upper limb [10]. Hand spasticity is called 'flexor synergy' which is characterized by flexion at the elbow, wrist, and finger joints combined with internal rotation and adduction of the shoulder [12, 13]. This causes unequal forces between the agonist and antagonist muscles of the upper limbs resulting in the static joint position and dynamic limb movements [12]. Neglecting to treat upper limb spasticity results in contractures due to abnormal shortening of the soft tissue structures surrounding the joints such as joint capsules, ligaments; tendons; muscles, and the skin [14]. mobilization and spasticity resulting in musculoskeletal tightness which decreases the functional recovery of the hand [15]. When left in the immobilized state with the flexor synergy; the condition of the upper limbs progresses to a fibrotic state which triggers the development of early contractures [15]. Pain: fibrosis, contracture, movement disorders, and muscle weakness usually accompanied by spasticity.

One of the rehabilitation treatments in stroke patients is using dynamic splints to reduce spasticity of the Hand and maintain muscle tissue length [16], It increases joint range of motion by providing a low-load prolonged timed tissue stretch. Dynamic splints can improve hand function by maintaining the peripheral muscle and joint structures at a functional length [15]. Hand mobility should be facilitated by using dynamic splints which stretch the muscles; tendons and ligaments to maintain their length, so reducing spasticity [14]. Spasticity and impaired hand motor skills can be treated by harnessing the plasticity property of the brain through mass movement and task-oriented arm training [14]. Hand splints can be used to train motor learning and improve neural plasticity in the brain [15]. Using a soft robotic glove as an assistive device was studied before [17–21]. Different wearable hand robots have been developed recently to assist hand function. Soft robotic gloves, exoskeletons lightweight, and low-cost were developed for hand rehabilitation after stroke [22, 23].

In recent years, there has been a growing interest in developing innovative technologies to revolutionize stroke rehabilitation. Among these advancements, the integration of wearable devices and artificial intelligence (AI) techniques has shown promise in creating personalized and effective rehabilitation strategies.[24–31]Specifically, the utilization of dynamic glove-based rehabilitation systems empowered by Convolutional Neural Networks (CNNs) presents a novel approach to address the challenges associated with spastic hands post-stroke.

The integration of CNN technology into the rehabilitation system enables continuous learning and adaptation. By analyzing patterns in hand movements and muscle responses, the CNN algorithm can dynamically adjust the rehabilitation regimen, optimizing the therapy's effectiveness over time. Moreover, the system's user-friendly interface and interactive feedback mechanisms engage stroke survivors actively in their rehabilitation journey, promoting motivation and adherence to the prescribed exercises.[32–34]

2. Methodology:

The smart rehabilitation system consists of biometric measurement gloves, rehabilitation gloves, a camera, a telecom unit, and a computer unit. **Figure 1** shows the block diagram of the smart rehabilitation system.

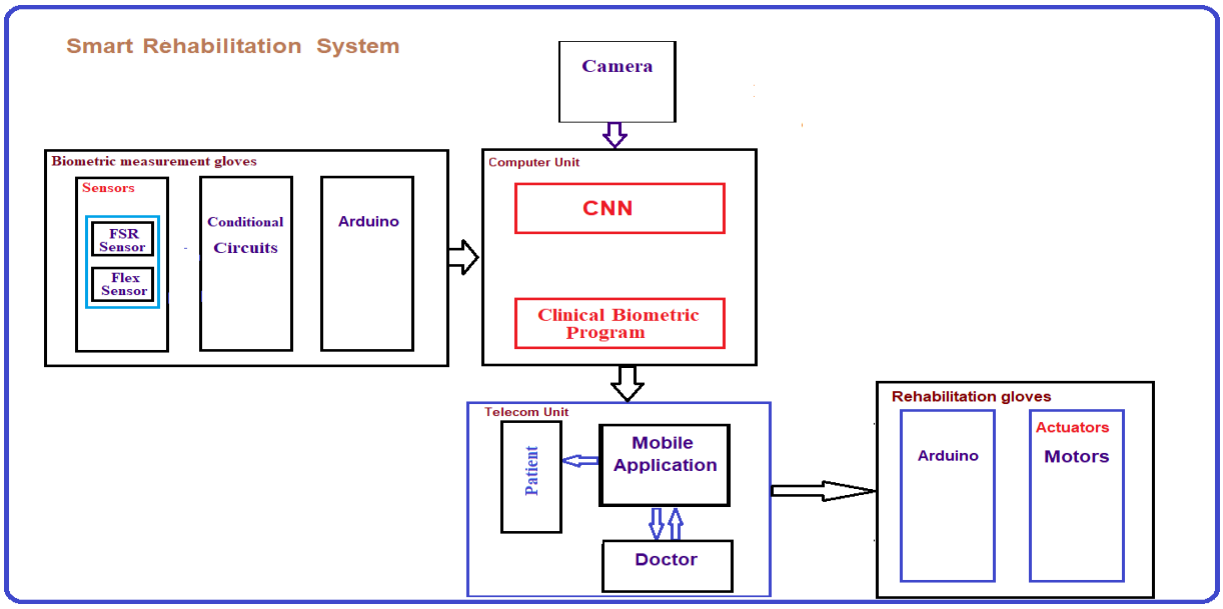

Figure 1: The block diagram of the smart rehabilitation system.

2.1. Biometric measurement gloves

Biometric measurement gloves consist of biometric sensors, conditional circuits, and Arduino Mega.

2.1.1. biometric sensors

Force-sensitive resistor (FSR) sensors and Flexible (Flex) sensors are two types of sensors in which the system is used to measure biometric measurements.

An electrical signal is produced by an FSR, a transducer that transforms mechanical forces like weight, pressure, and compression. The resistance of the sensor reduces with increasing force applied to it. The output resistance decreases as pressure increases.

Flex sensors or bend sensors are sensors whose resistance varies with the degree of bend or flexing movements they experience. They translate the change in bend into electrical resistance, the greater the bend, the higher the resistance value. There are five flex sensors and five FSR sensors used for each glove.

2.1.2. Conditional circuits

The FSR and Flex sensor outputs are resistance measurements corresponding to biometric measurements. They must be transformed into voltage signal outputs that will be used with Arduino inputs. To convert resistance output to voltage output, a voltage potential divider is used [35]. potential divider converts the change in resistance into a change in voltage. **Figure 2** shows the potential divider circuit and Equation 1 calculates the voltage output.

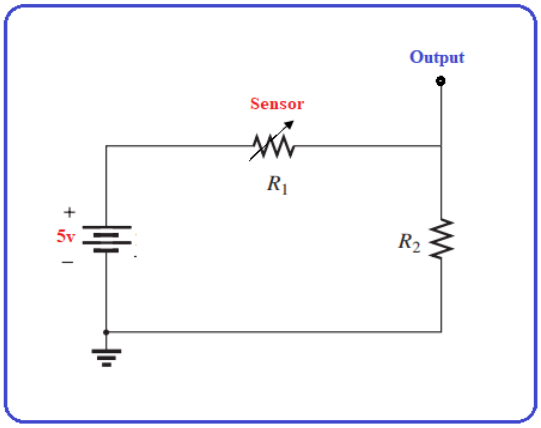

Figure 2: Potential divider circuit.

$$V_{out} = \frac{R_2}{R_1+R_2} V_{in} \quad = \frac{R_2}{R_1+R_2} 5\ V \quad \ldots\ldots\ldots\ldots\ldots\ldots(1)$$

Figure 3 (a,b) shows the conditional circuits of the FSR and Flex sensors respectively.

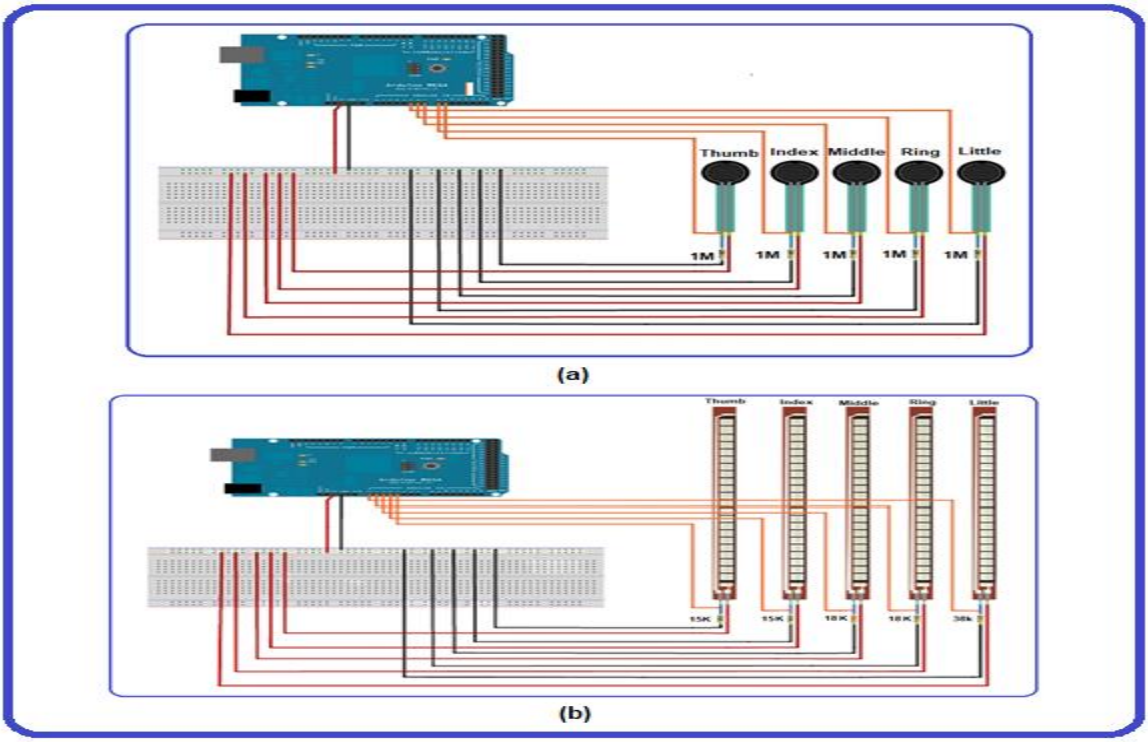

Figure 3: (a): The circuits of the FSR sensor, and (b): The circuits of the Flex sensor.

2.1.3. Arduino

After conditional circuits, the output voltage is the input to Arduino which converts it to digital voltage [36]. Analog readings are transformed to digital values between 0 and 1023 using Arduino's 10-bit analog-to-digital converter, which corresponds to the output range[37].

2.2. Computer unit:

This is the most important stage which is capable of receiving the data, analyzing it, and making a suitable decision.

2.2.1. Data inputs

This stage can accept two types of data which came from biometric measurements from sensors and a camera sensor. Biometric measurement gloves are measuring the features of the patients.

Table 1 (a,b) shows the features measurement of healthy and patient samples.

The second data input comes from the camera sensor. The SONY Cyber-shot DSC-W710 color digital camera was utilized for the experiments that were carried out for this system. The distance between the camera and the item was 0.4 m. Using the camera calibration approach, the camera was calibrated [38, 39]. The photos were recorded at a resolution of 2304 x 1728 pixels, however, they were downsized to 224 x 224 pixels. **Figure 4** shows four input images of healthy and patient persons which are taken by camera sensor.

Table 1: The features measurement of health and patients.

(a): Healthy Measurments

Number	FSR Sensor					Felx Sensor				
	Thumb	Index	Middle	Ring	Little	Thumb	Index	Middle	Ring	Little
H1	12	21	15	18	12	93	92	90	99	99
H2	14	25	16	21	16	93	92	93	99	98
H3	14	24	16	20	14	93	93	89	99	94
H4	13	23	17	18	14	92	93	90	99	95
H5	14	24	15	20	14	92	93	92	99	98
H6	13	24	16	19	14	92	93	89	99	99
H7	12	25	16	18	11	92	93	89	99	99
H8	12	22	15	18	12	91	92	92	94	99
H9	15	25	18	20	17	91	92	90	98	99
H10	14	22	17	17	12	91	91	88	95	99
H11	12	23	17	18	13	91	91	90	97	99
H12	13	24	17	19	15	90	90	89	96	99
H13	13	23	17	17	13	90	90	87	99	99
H14	13	23	16	18	13	90	90	88	99	99
H15	13	24	17	19	15	90	88	88	99	99

(b): Patients Measurments

Number	FSR Sensor					Felx Sensor				
	Thumb	Index	Middle	Ring	Little	Thumb	Index	Middle	Ring	Little
p1	31	35	35	32	31	11	10	11	11	10
p2	30	35	36	32	32	12	10	12	10	9
p3	30	36	36	32	32	12	10	15	11	9
p4	30	36	36	32	32	12	10	12	11	11
p5	30	35	36	32	32	11	9	12	10	9
p6	27	26	28	27	28	15	16	14	14	11
p7	31	36	36	32	32	12	11	13	13	11
p8	31	36	36	32	32	15	10	12	16	12
p9	35	32	32	31	30	12	10	14	15	15
p10	31	37	36	32	32	11	11	14	14	12
p11.	32	36	36	32	32	12	15	12	11	13
p12	38	36	36	32	32	12	14	14	14	14
p13	38	40	40	39	40	14	11	14	12	12
p14	31	36	36	32	32	13	10	15	11	14
p15	31	37	36	32	32	14	11	14	13	12

Healthy (H)
Patient (P)

Figure 4: (a,b) Images of healthy hands, and (c,d) images of patient hands according to Institutional Review Board (IRB), Faculty of Medicine, Minia University, Egypt (protocol: 403/10/2023).

2.3. Computer programs

There are two types of programs used in this stage; a clinical biometric program and a CNN program.

2.3.1. Clinical biometric program

It is a simple and linear program that can analyze biometric data and make decisions. The clinical biometric program is divided into two branches. The first one is a simple and designed to make decisions by using nested if conditions, and the second of them is designed to compute and analyses data using statistical analyses. **Figure 5** illustrates the flowchart of the clinical biometric program.

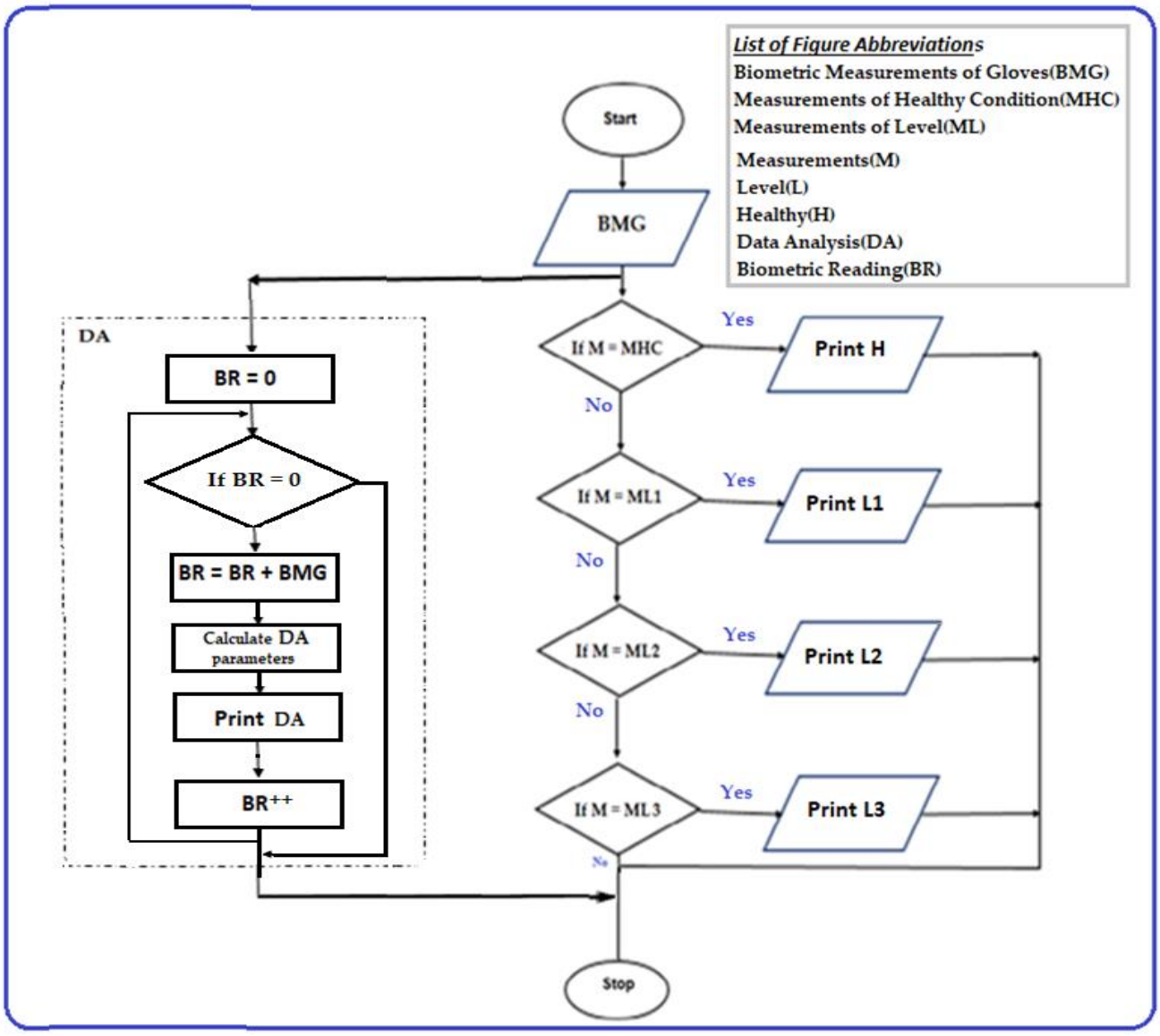

Figure 5: The flowchart of the clinical biometric program**.**

2.3.2. Deep Learning Model

A CNN is used to classify and diagnose spastic hand illnesses and disabilities diseases using imaging. To train a network, it convolutionally combines four different imaging classes(healthy and three levels of hand disabilities) by using 400 images which can be obtained from IRB of the Faculty of Medicine, Minia University, Egypt to introduce the idea of this research. The three categories of illnesses and disabilities of patients are demonstrated according to their reading from biometric measurements.

Figure 6 shows the three categories of illnesses and disabilities of patients according to biometric measurements.

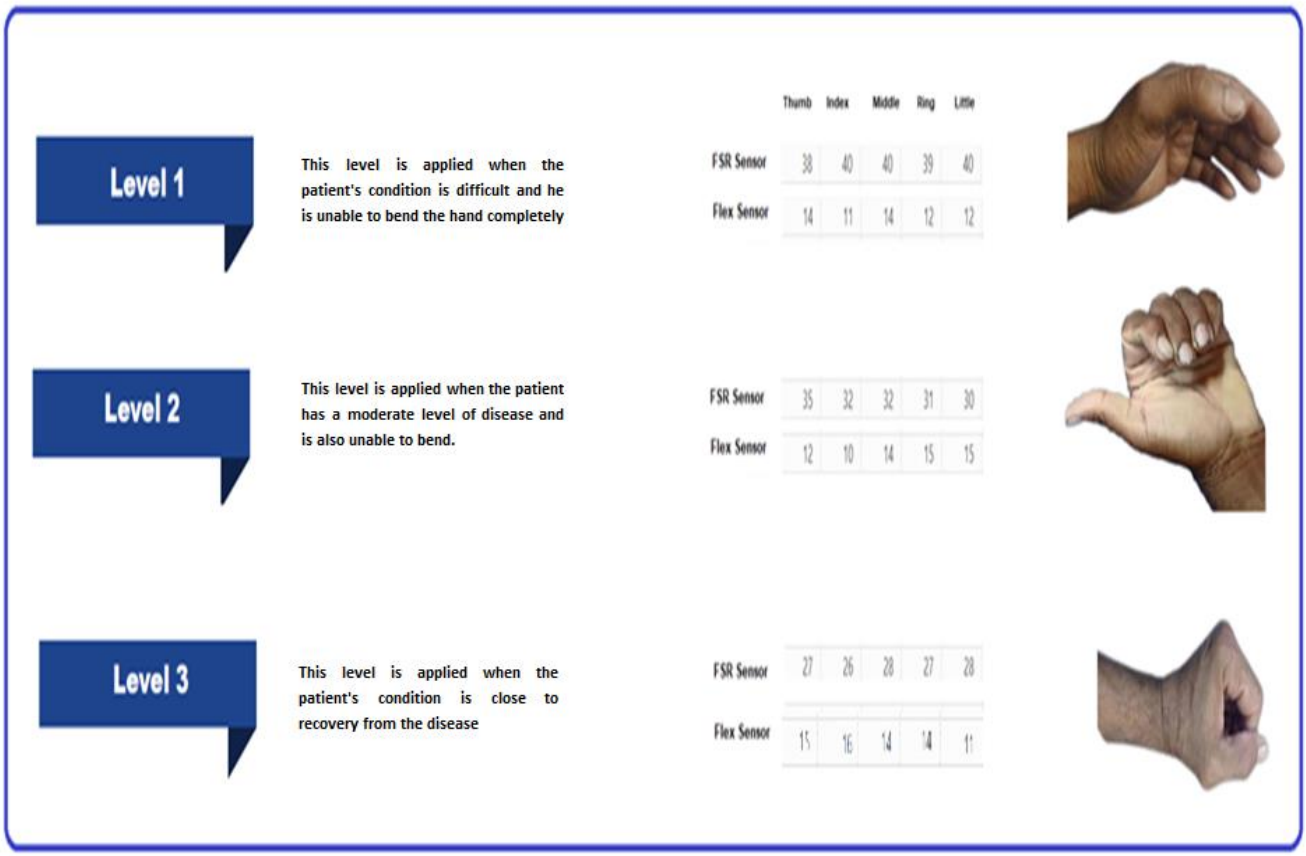

Figure 6: Three categories of disabilities according to biometric measurements.

The feature extractors and the classifier make up the two main components of the architecture of the proposed CNN. As the network expands, so does the CNN layer design. Each layer's number of retrieved features and the number of filters are associated. The following equation can be used to compute the feature map size [40]:

$$\text{Feature map size} = 1+(W-F+2P)/S \quad (2)$$

Where: W, F, P, and S are input size, filter size, stride, and padding respectively.

The deep convolutional neural network employed in this system is called ResNet50. It is a deep convolutional neural network with representative image auto-encoding and classification. The network in the classifier stage is built using a 50-layer residual network architecture, 5-fold cross-validation on four classification groups, 224x224x3-pixel images, 30 epochs, 6 iterations per epoch, and an Adam optimizer with a learning rate of 0.01. The training and testing processes are sped up using Residual50, which also increases accuracy overall and lowers error rates.

2.4. The ResNet50 architecture:

The ResNet50 architecture comprises four primary components: convolutional layers, identity blocks, convolutional blocks, and fully connected layers. These elements serve distinct functions within the network. The convolutional layers extract features from the input image, while the identity and convolutional blocks handle the processing and transformation of these features. Ultimately, the fully connected layers are employed to carry out the final classification process.

The ResNet50 model utilizes convolutional layers comprising multiple convolutional layers, accompanied by batch normalization and ReLU activation. These layers function to extract various features from the input image, including edges, textures, and shapes. Subsequently, max-pooling layers are employed after the convolutional layers, aiming to decrease the spatial dimensions of the feature maps while retaining the crucial features within them.

The primary components forming ResNet50 are the identity block and convolutional block. The identity block functions as a basic unit by directing the input through multiple convolutional layers and then reinstating the input to the resulting output. This mechanism enables the network to understand residual functions, aiding in mapping the input to the intended output. On the other hand, the convolutional block resembles the identity block but includes an extra 1x1 convolutional layer to decrease the number of filters before employing the 3x3 convolutional layer.

The concluding segment of ResNet50 comprises the fully connected layers, which play a pivotal role in executing the ultimate classification. These specific layers are accountable for determining the final categorization. The ultimate result of the last fully connected layer undergoes processing through a SoftMax activation function, ultimately generating the probabilities associated with each class**.** According to the tutorial study illustrated in [41] and its summary we select resnet type. Moreover, the resnet50 has a simple architecture and reduces the time of training with a good performance compared with other types of resnent. **Figure 7Figure 8** show the Residual50 architecture, and building of Resnet 50 respectively.

Resnet 50

layer name	output size	*(Resnet 50)*	Numbe of layers
conv1	112×112	7×7, 64, stride 2	**1**
conv2_x	56×56	3×3 max pool, stride 2	
		$\begin{bmatrix} 1\times1, 64 \\ 3\times3, 64 \\ 1\times1, 256 \end{bmatrix} \times3$	**9**
conv3_x	28×28	$\begin{bmatrix} 1\times1, 128 \\ 3\times3, 128 \\ 1\times1, 512 \end{bmatrix} \times4$	**12**
conv4_x	14×14	$\begin{bmatrix} 1\times1, 256 \\ 3\times3, 256 \\ 1\times1, 1024 \end{bmatrix} \times6$	**18**
conv5_x	7×7	$\begin{bmatrix} 1\times1, 512 \\ 3\times3, 512 \\ 1\times1, 2048 \end{bmatrix} \times3$	**9**
	1×1	average pool, 1000-d fc, softmax	**1**
FLOPs		3.8×10^9	50- layers

Figure 7: Residual50 architecture.

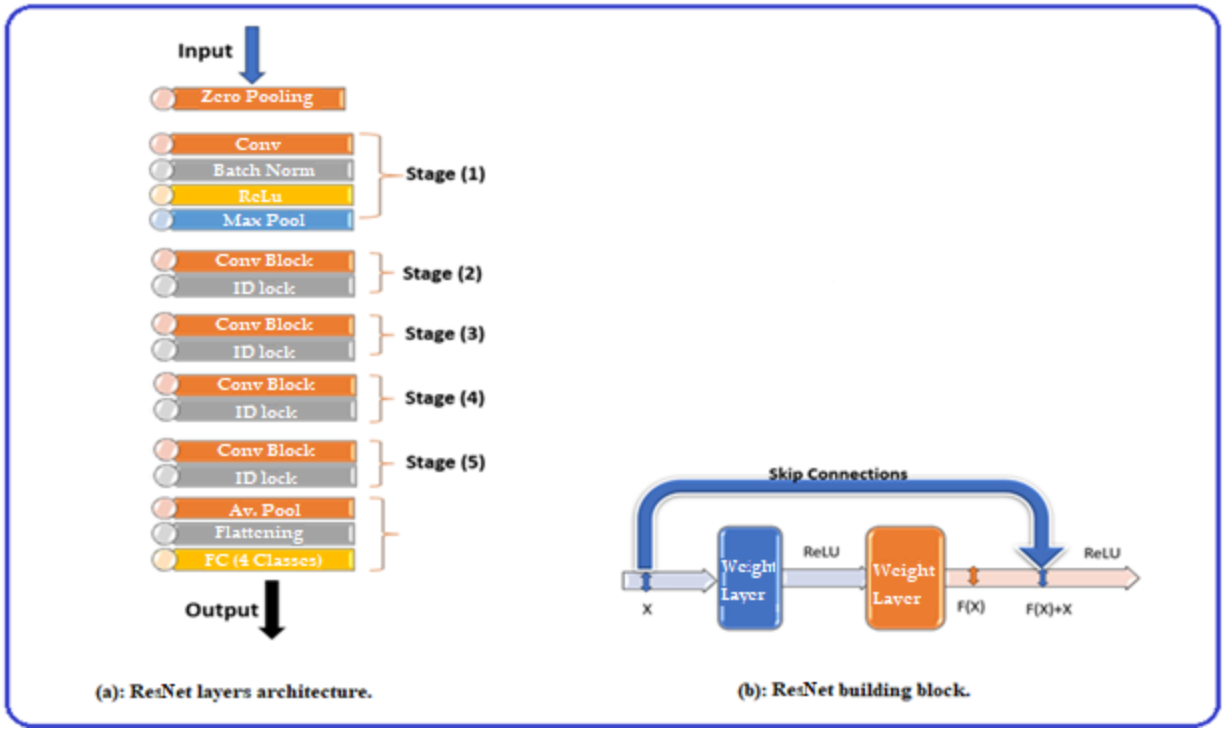

Figure 8: The architecture and building of ResNet 50, (a): ResNet layers architecture, and (b): ResNet building block.

Skip connections, alternatively referred to as residual connections, represent a crucial component within the ResNet50 framework. Their purpose is to enable the network to grasp more complex architectures while circumventing the issue of gradients vanishing, ensuring effective learning in deeper layers. The issue of vanishing gradients arises during the training of deep neural networks, wherein the gradients of parameters within the deeper layers diminish significantly, posing a challenge for these layers to effectively learn and enhance their performance. This difficulty escalates notably with the increased depth of the network. Skip connections resolve this issue by enabling direct information flow from the network's input to its output, circumventing certain layers. This capability empowers the network to acquire residual functions, effectively guiding the transformation of input into the desired output, without the necessity of learning the complete mapping process from the ground up.

ResNet50 incorporates skip connections within both the identity and convolutional blocks. In the identity block, the input undergoes convolutional layers and is subsequently merged with the output. Meanwhile, the convolutional block applies a 1x1 convolutional layer to diminish filter count before a 3x3 convolutional layer, then merges the input with the output.

The integration of skip connections in ResNet50 permits the network to grasp intricate architectures without encountering challenges in effective training or the occurrence of vanishing gradients. This mechanism enables the model to learn deeper structures while maintaining training efficiency.

2.5. Telecom unit

This unit is responsible for arriving at the health program decision from the computer unit to rehabilitation gloves, a doctor section, and a patient section as shown in Figure 1. Bluetooth HC-05 module is used for transparent wireless connection setup in this system. This module is interfaced with an Arduino controller. **Figure 9** shows the circuit of interfacing between the module and the Arduino controller.

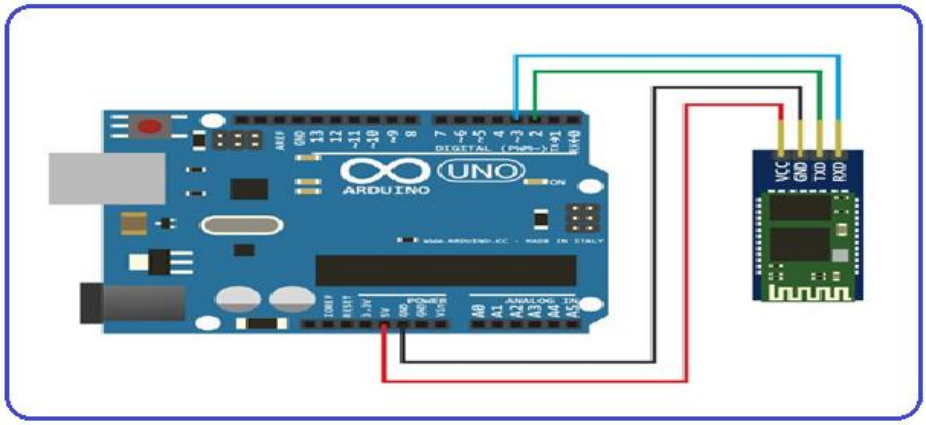

Figure 9: The interface between the Bluetooth module and Arduino.

The Telecom unit consists of mobile applications, the two sections, and a rehabilitation gloves, unit which were mentioned before. The mobile application for this system was designed by using the RemoteXY program.

In the first section, a patient can get message data from a system or a doctor, and sorts of these data can be used in an application to carry out a rehabilitation program.

A doctor has the power to change the rehabilitation choice that was generated by the computer programs in the second section.

The computer system's chosen rehabilitation program is sent to the rehabilitation gloves via a mobile application. The mobile application's home page and rehabilitation decision are depicted in **Figure 10**.

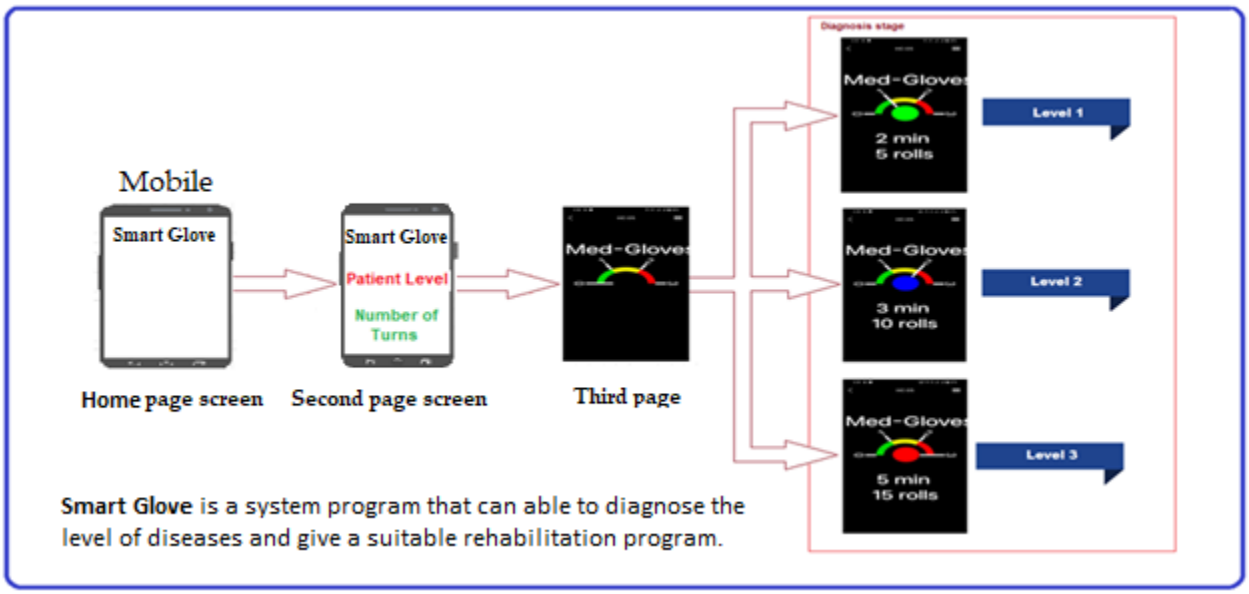

Figure 10: The mobile application's home page and rehabilitation decision.

2.6. Rehabilitation gloves

Rehabilitation gloves are responsible for actuating and helping the patient with hand exercises and therapies. It consists of Arduino, 5 servo motors, and wire connections. According to the diagnosis class or level which is decided by the computer unit, the rehabilitation gloves execute the therapy program. Moreover, in the telecom unit, a doctor has the authority to change the number of roles in therapy programs, if the case patient needs it. There are three levels and roles of execution that are demonstrated in **Figure 10**.

2.7. Arduino

It is a microcontroller that is able to execute the therapy program.

2.7.1. Servo motors

There are five servo motor types MG995 high-speed metal gear dual bpatientsrings used in this system. The motors are assistance devices that actuate patients with hand exercises.

2.7.2. wire connections

Polylactic Acid (PLA) is a wire connection that is used to connect between servo motors and gloves. It is a biodegradable, sustainable, and food-safe polymer made from organic sources so it was recommended to use in biomedical devices. Figure 11 shows the rehabilitation glove components and the smart rehabilitation system units mentioned in **Figure 11**.

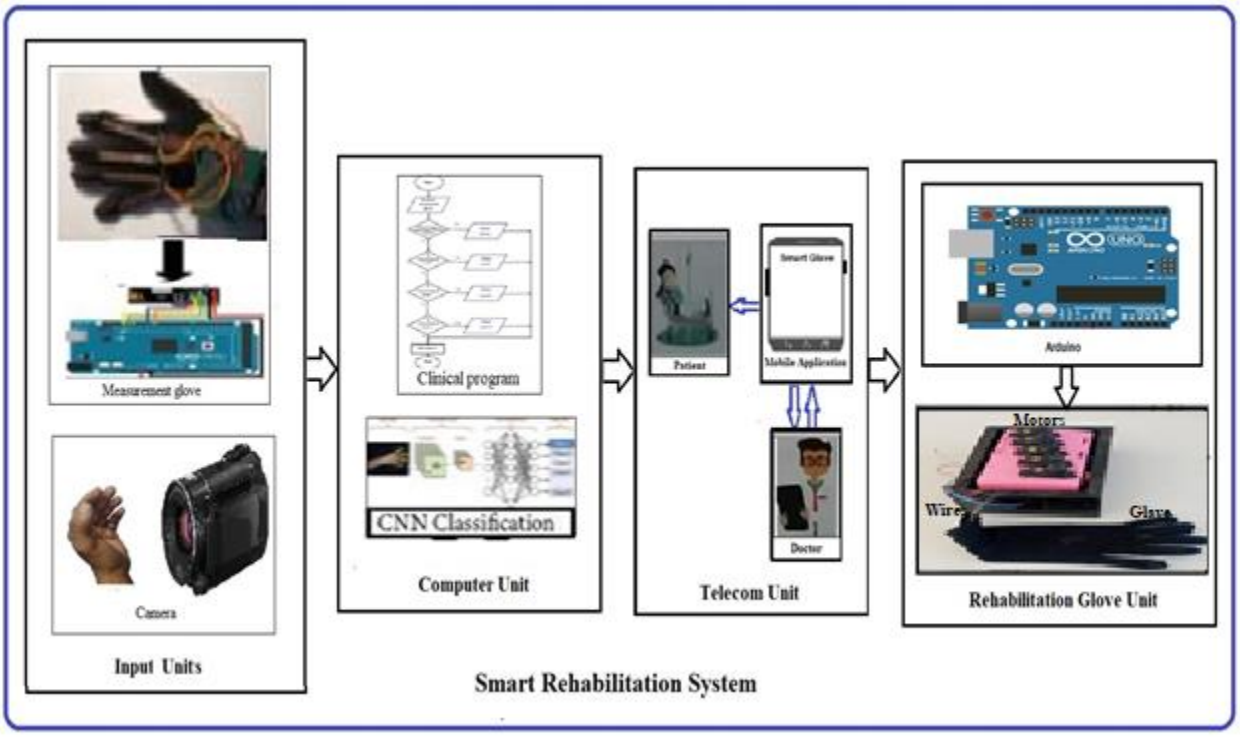

Figure 11: The smart rehabilitation system.

3. Results

3.1. Studies on human subjects

The Purdue Institutional Review Board (IRB), Faculty of Medicine, Minia University, Egypt (protocol-approval number: 403/10/2023) approved all experiments involving human subjects.

The results regarding the clinical biometric program are shown in **Table 2, Figure 12** illustrates the statistical graphs of biometric gloves.

Table 2: Statistical analysis of biometric hand measurements for patients and healthy persons.

Statistical Analysis	FSR Sensor					Felx Sensor				
	Thumb	Index	Middle	Ring	Little	Thumb	Index	Middle	Ring	Little
	12	21	15	18	12	93	92	90	99	99
	14	25	16	21	16	93	92	93	99	98
	14	24	16	20	14	93	93	89	99	94
	13	23	17	18	14	92	93	90	99	95
	14	24	15	20	14	92	93	92	99	98
	13	24	16	19	14	92	93	89	99	99
	12	25	16	18	11	92	93	89	99	99
	12	22	15	18	12	91	92	92	94	99
	15	25	18	20	17	91	92	90	98	99
	14	22	17	17	12	91	91	88	95	99
	12	23	17	18	13	91	91	90	97	99
	13	24	17	19	15	90	90	89	96	99
	13	23	17	17	13	90	90	87	99	99
	13	23	16	18	13	90	90	88	99	99
	13	24	17	19	15	90	88	88	99	99
	31	35	35	32	31	11	10	11	11	10
	30	35	36	32	32	12	10	12	10	9
	30	36	36	32	32	12	10	15	11	9
	30	36	36	32	32	12	10	12	11	11
	30	35	36	32	32	11	9	12	10	9
	27	26	28	27	28	15	16	14	14	11
	31	36	36	32	32	12	11	13	13	11
	31	36	36	32	32	15	10	12	16	12
	35	32	32	31	30	12	10	14	15	15
	31	37	36	32	32	11	11	14	14	12
	32	36	36	32	32	12	15	12	11	13
	38	36	36	32	32	12	14	14	14	14
	38	40	40	39	40	14	11	14	12	12
	31	36	36	32	32	13	10	15	11	14
	31	37	36	32	32	14	11	14	13	12
Average	22.43333	29.36667	25.86667	25.36667	22.86667	51.96667	51.36667	51.4	55.2	54.93333
Mode	13	36	36	32	32	12	10	14	99	99
Median	21	25.5	23	24	22.5	52.5	52	51	55	54.5
standard deviation	9.708451	6.413796	9.877642	7.049007	9.579912	40.12608	40.89219	38.88054	43.56715	44.10718
variance	94.25402	41.13678	97.56782	49.68851	91.77471	1610.102	1672.171	1511.697	1898.097	1945.444

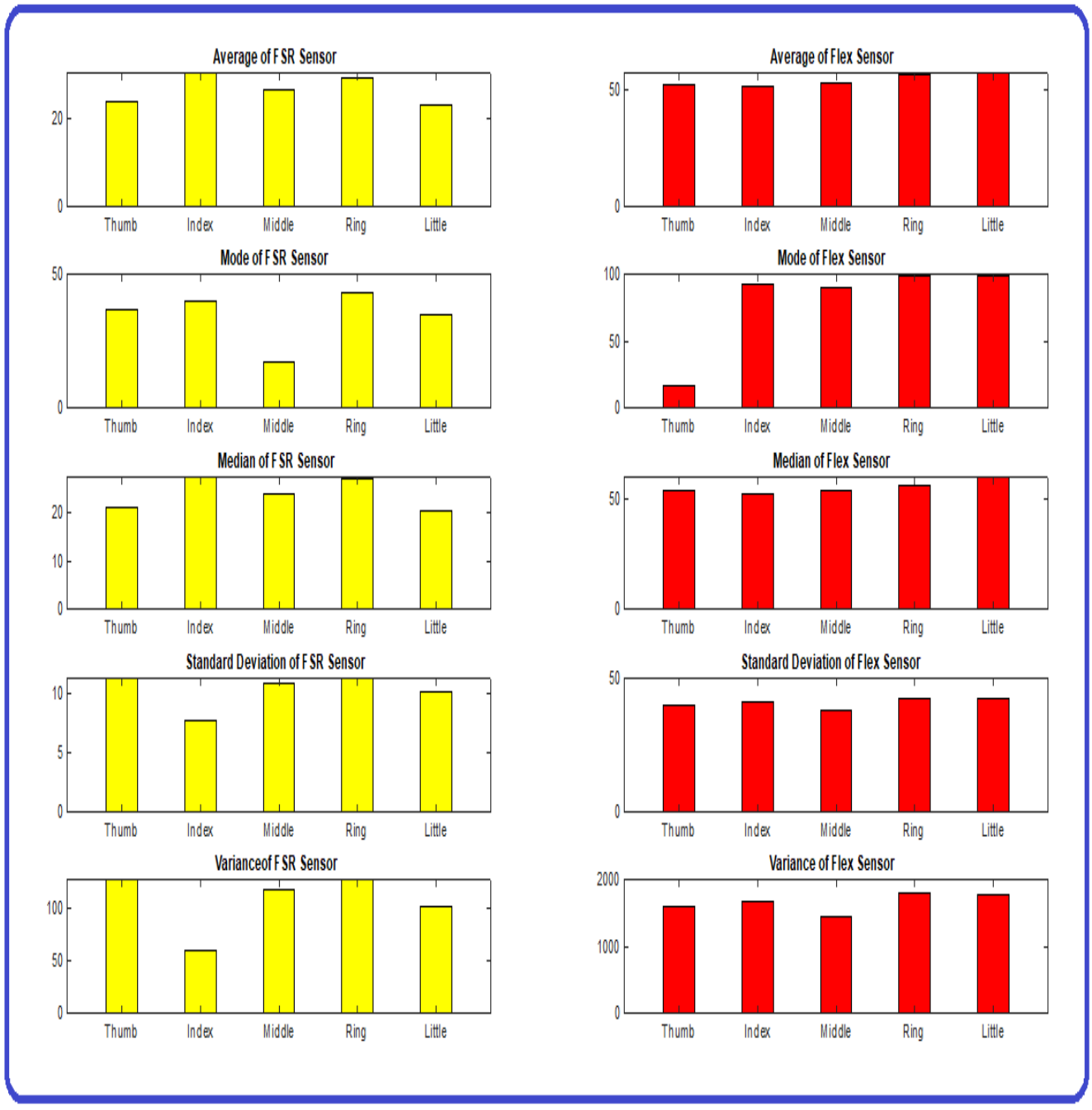

Figure 12 Statistical graphs of biometric gloves.

3.2. The results of the CNN program:

ResNet50 demonstrated 177 layers with 23.5M total learnable and accuracy = 0.9901. The system's accuracy and loss training curves are shown in **Figure 13**.

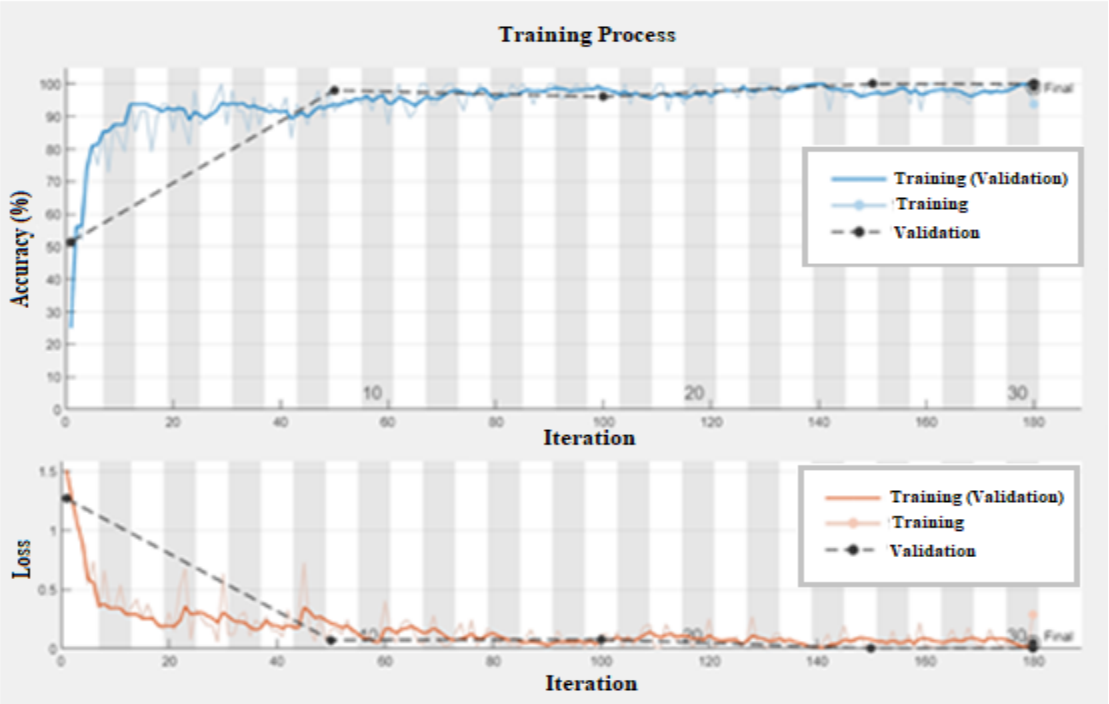

Figure 13: The training curves of accuracy and loss training carves.

3.3. Confusion matrix:

The confusion matrix is used to evaluate the system's performance. The confusion matrix parameters and evaluation metrics are illustrated in **Figure 14,**

Table 3 shows the results of the training table according to the number of epochs.

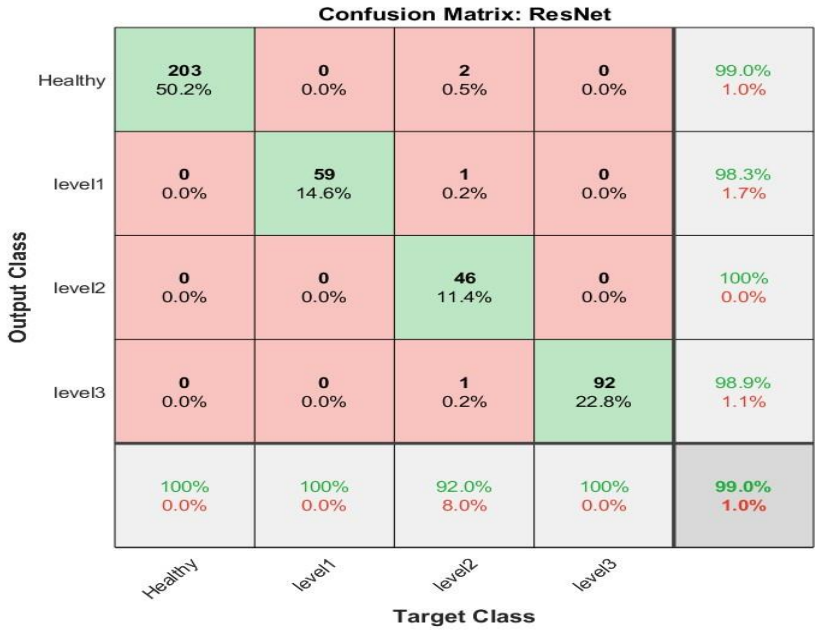

Figure 14: The confusion matrix.

Table 3: The results of training table according to the number of epochs.

Training on single GPU.
Initializing input data normalization.

Epoch	Iteration	Time Elapsed (hh:mm:ss)	Mini-batch Accuracy	Validation Accuracy	Mini-batch Loss	Validation Loss	Base Learning Rate
1	1	00:00:41	25.00%	51.49%	1.5133	1.2691	0.0100
9	50	00:18:08	91.67%	98.02%	0.1631	0.0728	0.0100
17	100	00:36:10	95.83%	96.04%	0.1186	0.0768	0.0100
25	150	00:53:36	100.00%	100.00%	0.0201	0.0035	0.0100
30	180	01:03:59	93.75%	100.00%	0.2895	0.0053	0.0100

4. Conclusion

This study introduces an innovative rehabilitation system tailored for diagnosing and addressing spastic hand conditions. The system incorporates two specialized glove types: biometric measurement gloves for patient feature assessment and rehabilitation gloves for facilitating hand exercises and therapies. The diagnostic process employs two programs: a clinical biometric program utilizing data from the biometric gloves, and an intelligent CNN-based program designed to identify optimal rehabilitation therapies via camera-captured images. The system's diverse data inputs afford it a robust advantage, with the CNN achieving an impressive validation accuracy rate of 100 % and validation loss of 0.0053 after 180 iterations with about one hour time of processing using one GPU in classifying and recommending rehabilitation programs based on image analysis.

Central to its functionality is a mobile application facilitating seamless communication between the system, patients, and healthcare providers. Notably, this smart rehabilitation system boasts several advantages, including user-friendly operation without external assistance, cost-effectiveness, elimination of the need for physical visits to rehabilitation centers, and exceptional accuracy attributed to the utilization of AI within the CNN framework.

References

[1] M. P. Lindsay *et al.*, "World Stroke Organization (WSO): Global Stroke Fact Sheet 2019," *International Journal of Stroke*, vol. 14, no. 8, pp. 806–817, Oct. 2019, doi: 10.1177/1747493019881353.

[2] W. Rosamond *et al.*, "Heart Disease and Stroke Statistics—2008 Update," *Circulation*, vol. 117, no. 4, 2008, doi: 10.1161/circulationaha.107.187998.

[3] S.-M. Lai, S. Studenski, P. W. Duncan, and S. Perera, "Persisting Consequences of Stroke Measured by the Stroke Impact Scale," *Stroke*, vol. 33, no. 7, pp. 1840–1844, Jul. 2002, doi: 10.1161/01.STR.0000019289.15440.F2.

[4] M. N. Bartels, C. A. Duffy, and H. E. Beland, "Pathophysiology, Medical Management, and Acute Rehabilitation of Stroke Survivors," *Stroke Rehabilitation*. Elsevier, pp. 2–45, 2016. doi: 10.1016/b978-0-323-17281-3.00001-0.

[5] A. Thibaut, C. Chatelle, E. Ziegler, M.-A. Bruno, S. Laureys, and O. Gosseries, "Spasticity after stroke: Physiology, assessment and treatment," *Brain Inj*, vol. 27, no. 10, pp. 1093–1105, 2013, doi: 10.3109/02699052.2013.804202.

[6] N. Venketasubramanian, A. Yin, L. B. Lee, and D. A. De Silva, "Two decades of nation-wide community-based stroke support – The Singapore National Stroke Association," *International Journal of Stroke*, vol. 12, no. 3, pp. 297–301, 2016, doi: 10.1177/1747493016676620.

[7] G. M. Johansson, "Clinical and kinematic assessments of upper limb function in persons with post-stroke symptoms," Umeå universitet, Physiotherapy, Department of Community Medicine and Rehabilitation, Faculty of Medicine, Umeå University, 2015.

[8] A. Leo *et al.*, "Spasticity Management: The Current State of Transcranial Neuromodulation," *PM&R*, vol. 9, no. 10, pp. 1020–1029, 2017, doi: 10.1016/j.pmrj.2017.03.014.

[9] B. Atchison and D. K. Dirette, *Conditions in occupational therapy: Effect on occupational performance*. Lippincott Williams & Wilkins, 2007.

[10] P. Raghavan, "Upper Limb Motor Impairment After Stroke," *Phys Med Rehabil Clin N Am*, vol. 26, no. 4, pp. 599–610, Nov. 2015, doi: 10.1016/j.pmr.2015.06.008.

[11] JamesW. Lance, "What is spasticity?," *The Lancet*, vol. 335, no. 8689, p. 606, 1990, doi: 10.1016/0140-6736(90)90389-m.

[12] A. Naro *et al.*, "Breakthroughs in the spasticity management: Are non-pharmacological treatments the future?," *Journal of Clinical Neuroscience*, vol. 39, pp. 16–27, 2017, doi: 10.1016/j.jocn.2017.02.044.

[13] "Evidence Base of Stroke and Hand Splinting," *International Journal of Science and Research (IJSR)*, vol. 5, no. 2, pp. 2014–2017, Feb. 2016, doi: 10.21275/v5i2.NOV161521.

[14] Saebo, "The Benefits of Dynamic Splints and Rehabilitation Gloves for Stroke Recovery," medium. [Online]. Available: https://medium.com/@saebooutreach/the-benefits-of-dynamic-splints-and-rehabilitation-gloves-for-stroke-recovery-3d3d5d3a15cc

[15] D. Greg Pitts and S. Peganoff O'Brien, "Splinting the Hand to Enhance Motor Control and Brain Plasticity," *Top Stroke Rehabil*, vol. 15, no. 5, pp. 456–467, 2008, doi: 10.1310/tsr1505-456.

[16] T. Rowland, D. Cooke, and L. Gustafsson, "Role of occupational therapy after stroke," *Ann Indian Acad Neurol*, vol. 11, no. 5, p. 99, 2008, doi: 10.4103/0972-2327.41723.

[17] H. K. Yap, J. H. Lim, F. Nasrallah, and C.-H. Yeow, "Design and Preliminary Feasibility Study of a Soft Robotic Glove for Hand Function Assistance in Stroke Survivors," *Front Neurosci*, vol. 11, Oct. 2017, doi: 10.3389/fnins.2017.00547.

[18] A. L. van Ommeren *et al.*, "The Effect of Prolonged Use of a Wearable Soft-Robotic Glove Post Stroke - a Proof-of-Principle," *2018 7th IEEE International Conference on Biomedical Robotics and Biomechatronics (Biorob)*. IEEE, 2018. doi: 10.1109/biorob.2018.8487906.

[19] B. Radder, G. Prange-Lasonder, A. Kottink, A. Melendez-Calderon, J. Buurke, and J. Rietman, "Feasibility of a wearable soft-robotic glove to support impaired hand function in stroke patients," *J Rehabil Med*, vol. 50, no. 7, pp. 598–606, 2018, doi: 10.2340/16501977-2357.

[20] A. Yurkewich *et al.*, "Myoelectric untethered robotic glove enhances hand function and performance on daily living tasks after stroke," *J Rehabil Assist Technol Eng*, vol. 7, p. 205566832096405, Jan. 2020, doi: 10.1177/2055668320964050.

[21] A. Yurkewich, I. J. Kozak, D. Hebert, R. H. Wang, and A. Mihailidis, "Hand Extension Robot Orthosis (HERO) Grip Glove: enabling independence amongst persons with severe hand impairments after stroke," *J Neuroeng Rehabil*, vol. 17, no. 1, p. 33, Feb. 2020, doi: 10.1186/s12984-020-00659-5.

[22] B. B. Kang, H. Lee, H. In, U. Jeong, J. Chung, and K.-J. Cho, "Development of a polymer-based tendon-driven wearable robotic hand," *2016 IEEE International Conference on Robotics and Automation (ICRA)*. IEEE, 2016. doi: 10.1109/icra.2016.7487562.

[23] D. Popescu, M. Ivanescu, R. Popescu, L.-C. Popescu, A. Petrisor, and A.-M. Bumbea, "Post-stroke assistive rehabilitation robotic gloves," *2016 International Conference and Exposition on Electrical and Power Engineering (EPE)*. IEEE, 2016. doi: 10.1109/icepe.2016.7781363.

[24] O. Kossi, C. Batcho, T. Adoukonou, and J. Thonnard, "Functional recovery after stroke in Benin: A six-month follow-up study," *J Rehabil Med*, vol. 48, no. 8, pp. 671–675, 2016, doi: 10.2340/16501977-2128.

[25] C. D. Takahashi, L. Der-Yeghiaian, V. Le, R. R. Motiwala, and S. C. Cramer, "Robot-based hand motor therapy after stroke," *Brain*, vol. 131, no. 2, pp. 425–437, 2008, doi: 10.1093/brain/awm311.

[26] P. Polygerinos *et al.*, "Towards a soft pneumatic glove for hand rehabilitation," *2013 IEEE/RSJ International Conference on Intelligent Robots and Systems*. IEEE, 2013. doi: 10.1109/iros.2013.6696549.

[27] T. Yang and X. Gao, "Adaptive Neural Sliding-Mode Controller for Alternative Control Strategies in Lower Limb Rehabilitation," *IEEE Transactions on Neural Systems and Rehabilitation Engineering*, vol. 28, no. 1, pp. 238–247, 2020, doi: 10.1109/tnsre.2019.2946407.

[28] A. Elnady, W. Ben Mortenson, and C. Menon, "Perceptions of Existing Wearable Robotic Devices for Upper Extremity and Suggestions for Their Development: Findings From Therapists and People With Stroke," *JMIR Rehabil Assist Technol*, vol. 5, no. 1, pp. e12–e12, May 2018, doi: 10.2196/rehab.9535.

[29] M. Panwar *et al.*, "Rehab-Net: Deep Learning Framework for Arm Movement Classification Using Wearable Sensors for Stroke Rehabilitation," *IEEE Trans Biomed Eng*, vol. 66, no. 11, pp. 3026–3037, 2019, doi: 10.1109/tbme.2019.2899927.

[30] L. Montesinos, R. Castaldo, and L. Pecchia, "Wearable Inertial Sensors for Fall Risk Assessment and Prediction in Older Adults: A Systematic Review and Meta-Analysis," *IEEE Transactions on Neural Systems and Rehabilitation Engineering*, vol. 26, no. 3, pp. 573–582, 2018, doi: 10.1109/tnsre.2017.2771383.

[31] R. Santos, R. Correia, Y. Mazin, H. Andrade, and F. Quinaz, "A Pilot Study of an Innovative Hand Exoskeleton: Nuada Glove," *Cureus*, vol. 15, no. 10, pp. e47411–e47411, Oct. 2023, doi: 10.7759/cureus.47411.

[32] "IEEE Transactions on Neural Systems and Rehabilitation Engineering publication information," *IEEE Transactions on Neural Systems and Rehabilitation Engineering*, vol. 27, no. 10, pp. C2–C2, 2019, doi: 10.1109/tnsre.2019.2942794.

[33] Y. Lee, B. Lee, C. Lee, and M. Lee, "Implementation of Wearable Sensor Glove using Pulse-wave Sensor, Conducting Fabric and Embedded System," *2006 3rd IEEE/EMBS International Summer School on Medical Devices and Biosensors*. IEEE, 2006. doi: 10.1109/issmdbs.2006.360106.

[34] J. Zhang, D. Liu, and Q.-W. Tang, "The CNN Deep Learning-Based Melting Process Prediction of Czochralski Monocrystalline Silicon," *IEEE Access*, vol. 10, pp. 41986–41992, 2022, doi: 10.1109/access.2022.3168021.

[35] S. Sasidharan, "Smart glove: an assistive device to enhance recovery of hand function during motor rehabilitation," Arizona State University, 2015.

[36] T. Aghil, S. Rahul, S. B. Kumaar, Y. Vijay, S. T. Kumar, and B. Sidhharth, "A futuristic approach for stroke rehabilitation using smart gloves," in *Journal of Physics: Conference Series*, IOP Publishing, 2021, p. 12025.

[37] https://www.farnell.com/datasheets/1682209.pdf

[38] P. S. Herianto and A. Darmawan, "Development of digital anthropometric circumferential measurement system based on two-dimensional images," in *The 11th Asia Pacific Industrial Engineering and Management Systems Conference, Melaka*, 2010, pp. 7–10.

[39] M. Moness, S. K. Loutfy, and M. A. Massoud, "Selecting Promising Junior Swimmers in Egypt Using Automated Biometric Algorithms of Image Processing and Fuzzy Concepts," *IEEE Access*, vol. 9, pp. 89476–89496, 2021.

[40] https://medium.com/analytics-vidhya/convolutional-neural-networks-an-intuitive-approach-part-2-729bfb5e4d87.

[41] https://towardsdatascience.com/the-w3h-of-alexnet-vggnet-resnet-and-inception-7baaaecccc96